Performance Optimization and Stack Geometry Design in a Standing Wave Thermoacoustic Refrigerator

Amey S. Wagh¹, Muzammil Baig², Samir Chaudhary³, Naeem Chunre⁴, Wasi Ahmed⁵

¹Asstt. Professor, Dept. of Mechanical Engineering, M.H. Saboo Siddik College of Engineering, Mumbai, 400008, India.

^{2,3,4,5} UG- student, Dept. of Mechanical Engineering, M.H. Saboo Siddik College of Engineering, Mumbai, 400008. India.

Abstract: This study presents the design, construction, and evaluation of a prototype standing-wave thermoacoustic refrigerator (TAR) as a sustainable alternative to conventional vapor-compression cooling systems. Using a dimensional parameter design strategy, the TAR was fabricated with cost-effective and easily replaceable components. Helium was selected as the working fluid due to its favorable thermophysical properties, while a Kapton-based parallel-plate stack was optimized to achieve effective thermal-acoustic coupling. Experimental testing confirmed the creation of a measurable cooling effect below ambient temperature, although efficiency and cooling capacity remain modest. The prototype achieved a maximum coefficient of performance (COP) of 2.9 and a cooling capacity of 1.4 W with an input acoustic power of just under 0.5 W. These results highlight TAR's potential as an environmentally friendly technology, while also pointing to the need for refinement in stack geometry, operating frequency, and material selection to achieve practical applications.

Keywords: Thermoacoustic refrigeration (TAR), Standing-wave thermoacoustics, Stack geometry optimization, Eco-friendly refrigeration

I. INTRODUCTION

Refrigeration technologies are integral to industrial, commercial, and domestic sectors, yet traditional vapor-compression systems continue to raise environmental concerns due to their reliance on chlorofluorocarbons (CFCs) and hydrofluorocarbons (HFCs). The environmental consequences of these refrigerants, particularly in relation to ozone depletion and global warming, prompted international agreements such as the Montreal Protocol to phase them out. As a result, researchers have increasingly focused on alternative, green cooling methods (Raut & Wankhede, 2015). One promising approach is thermoacoustic refrigeration (TAR), which couple principles of acoustics and thermodynamics to enable cooling without harmful refrigerants or mechanical compressors (Swift, 2002; Radebaugh, 2009).

The concept of thermoacoustic phenomena was first qualitatively described by Lord Rayleigh in 1887. However, meaningful progress was not achieved until the late 20th century through the work of Rott, Hofler, and Swift (Hofler, 1986; Swift, 2002). Thermoacoustic refrigeration operates by utilizing sound waves to generate standing-wave pressure oscillations in a resonator, which in turn induce temperature gradients across a porous medium, known as the stack. When coupled with heat exchangers, this temperature gradient can be harnessed to create a cooling effect. Compared with vapor-compression systems, TAR systems are mechanically simpler, contain no moving parts, and use inert gases such as helium, making them inherently eco-friendly and robust against leakage (Olson et al., 2005; Jin et al., 2015).

II. LITERATURE REVIEW

Thermoacoustic refrigeration operates on the principle of converting acoustic energy into a temperature gradient using a standing-wave or traveling-wave configuration. In a standing-wave TAR, a driver such as a loudspeaker generates pressure oscillations within a resonator filled with an inert gas. These oscillations cause regions of compression and rarefaction, which in turn produce alternating heating and cooling effects due to adiabatic processes (Radebaugh, 2009). A porous medium, known as the stack, is placed at a strategic location in the resonator to facilitate heat transfer. Heat exchangers are positioned at both ends of the stack to extract heat from the cold side and reject it from the hot side, thus enabling refrigeration without conventional refrigerants (Olson et al., 2005).

The configuration of standing-wave thermoacoustic refrigerators is simple. A standing-wave TAR comprises of a driver, a resonator, and a stack. To make the device practical, it must also utilize two heat exchangers; however, they are not necessary for creating a temperature difference across the stack. The parts are assembled as shown in Figure 1

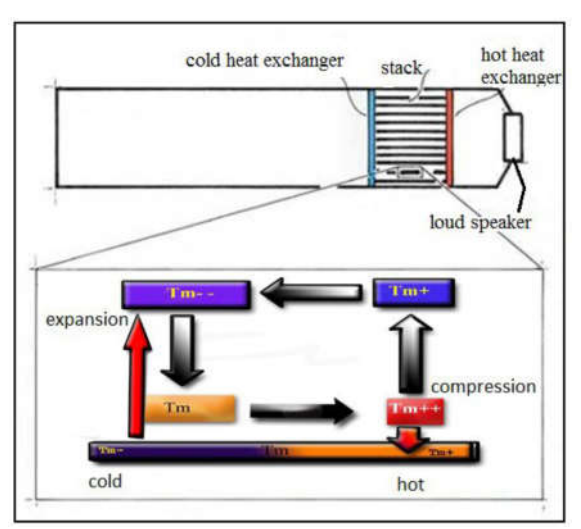


Fig 1. Simple illustration of Thermoacoustic Refrigerator and its working.

Traditional Vapor Compression refrigeration system involves the use of refrigerant which cause ozone depletion and harm the global environment. Whereas in case of TAR uses inert fluids which is safe and environment friendly in event if it is leaked and is mechanically simpler and has no moving parts as in case of conventional refrigeration system. The development of thermoacoustic refrigeration is driven by the possibility that it may replace current refrigeration technology.

III. METHODOLOGY

The research followed a structured process that combined theoretical analysis, design calculations, fabrication, and experimental testing. The overall aim was to develop a functional prototype of a standing-wave thermoacoustic refrigerator (TAR) and to evaluate its performance. The steps followed are:

- Selection of Working Fluid
- Operating Parameters
- Stack and Resonator Design
- Fabrication and Assembly
- Experimental Setup and Testing
- Performance Evaluation

IV. DESIGN OF STANDING WAVE TAR

In designing a standing-wave TAR, there are many parameters to consider, including the stack length and position, pore size and geometry, driver parameters, resonator dimensions, working gas properties, and operating conditions. To begin design, a few choices must be made to reduce the number of variables. Often the first step is selecting a working gas because it is much easier to design other parameters around the physical properties of a fluid than to find or create a fluid with the physical properties dictated by choosing other parameters first.

4.1 Working Gas

The working gas should be chosen to have a large thermal penetration depth (δ_k) and a small viscous penetration depth (δ_v) . Thermal penetration depth is a measure of how well a fluid can transfer heat through its boundary. A large thermal penetration depth allows for more heat transfer between the stack walls and the gas, increasing the overall efficiency of the TAR. A fluid's viscous penetration depth can be viewed as a measure of the frictional losses within the fluid. A small viscous penetration depth indicates that losses per unit area due to viscous effects will be lower, which is important in the many small pores of the stack where the surface area is large. The thermal and viscous penetration depths are related by a fluid's Prandtl number, defined as

$$\sigma = \frac{\delta_{\nu}^2}{\delta_{\nu}^2} \tag{1}$$

The thermal and viscous penetration depths are given by,

$$\delta_k = \sqrt{\frac{2K}{\rho c_p \omega}} \tag{2}$$

$$\delta_v = \sqrt{\frac{2\mu}{\rho\omega}} \tag{3}$$

Where K is the thermal conductivity, μ is the viscosity, ρ is the density, C_P is the isobaric specific heat of the gas, and ω is the angular frequency of the sound wave.

Helium was selected for its low Prandtl number (0.68), high thermal conductivity (0.138 W/m·K), and high specific heat ratio ($\gamma = 5/3$) [1]. Its low molecular weight minimizes viscous losses, while its thermal properties enable effective heat transfer. The working gas was maintained at atmospheric pressure (101 kPa) to avoid leakage challenges and reduce sealing costs [14].

Table 1. Properties of Helium.

K	0.138 W/(m*K)
γ	5/3
C_P	5193.2 J/(kg*K)
σ	0.68
$R_{\rm s}$	2077

4.2 Mean pressure

Since the power density in a thermoacoustic device is proportional to the mean pressure p_m , it is favorable to choose p_m as large as possible. This is determined by the mechanical strength of the resonator. Designing a stronger resonator often leads to more expensive materials and a heavier, bulkier overall TAR. On the other hand, δ_k is inversely proportional to square root of p_m , so a high pressure results in a small δ_k and small stack plate spacing. This makes the construction difficult. In addition to these drawbacks, a higher

internal pressure makes it more difficult to seal the working gas inside. Sealing the TAR can be especially problematic when working with helium due to its small molecular size. As cost was of some importance to the current endeavor, the mean pressure was chosen to be 1 atmosphere, or 101 kPa. Using atmospheric helium greatly reduced the risk of leakage thereby eliminating the need for expensive seal materials.

4.3 Frequency

As the power density in the thermoacoustic devices is a linear function of the acoustic resonance frequency an obvious choice is thus a high resonance frequency. On the other hand, δ_k is inversely proportional to the square root of the frequency which again implies a stack with very small plate spacing.

The operating frequency was set between 300–400 Hz to balance power density with manufacturability [12]. Higher frequencies increase power density but require smaller stack spacing, which complicates fabrication [20].

4.4 Drive ratio

The drive ratio D is defined as the acoustic pressure amplitude p_0 divided by the mean pressure p_m . This ratio should be kept sufficiently low so as to avoid acoustic nonlinearities such as turbulence. Specifically, the dimensionless Mach number, M, should be smaller than about 0.1, and the Reynolds number, Ry, should be smaller than 500. Tijani uses the following definition of the Mach number,

$$M = \frac{p_0}{\rho_m a^2} \tag{4}$$

Where a is the adiabatic speed of sound, and ρ_m is the density for the mean operating conditions; however, a more readily useable form was derived and is given by,

$$M = \frac{D}{\gamma} \tag{5}$$

This formulation seems to be better suited for use with the dimensionless equations in designing the stack. Given for γ =5/3, the drive ratio must be less than 16.7% to ensure that M<0.1 and less than 10.0% to ensure that Ry < 500. Because the chosen mean pressure is 101 kPa, the acoustic pressure amplitude must be less than 10 kPa, a large number for a normal loud speaker, the intended driver. The actual drive ratio for a loud speaker is more likely to be on the order of a few percent.

To avoid nonlinear acoustic effects, the drive ratio was set at D = 0.01, ensuring that the Mach number remained below 0.1 and the Reynolds number under 500 [19].

4.5 Stack

The stack is the most critical component of a thermoacoustic refrigerator, as minor dimensional changes can significantly impact performance [8]. It comprises closely spaced parallel surfaces aligned along the resonator's length, converting acoustic pressure oscillations into a temperature gradient [7]. For optimal performance, the stack material should exhibit low thermal conductivity and higher specific heat capacity than the working gas, while pore geometry must balance thermal efficiency with minimal viscous losses [11]. Stack length and position are determined using dimensionless heat and work flow equations [15].

4.5.1 Stack Material

Heat conduction through the stack material and the enclosed gas can degrade performance by reducing the temperature gradient [11]. Suitable materials include ceramics and plastics, chosen for their low thermal conductivity and manufacturability [5]. Ceramics often have desirable thermal properties but are brittle and challenging to machine [10], whereas plastics like Mylar, Melinex, and Kapton allow easier fabrication into spiral or parallel-plate configurations [11]. For this work, Kapton (polyimide) was selected due to its availability, low thermal conductivity (0.12 W/m·K), and low cost [16].

4.5.2 Stack Geometry

Pore geometry strongly influences the conversion of acoustic work into cooling power [20]. While pin arrays achieve the highest efficiency [8], they are complex to manufacture. Therefore, a parallel-plate configuration was adopted as a practical alternative [19].

4.5.3 Stack Pore Size

Pore size is determined by the thermal penetration depth, δk , which dictates heat transfer efficiency between the gas and stack walls [2]. Optimal stack spacing is 2–4 δk to maximize thermal contact without significantly disrupting the acoustic field [19]. Using $\delta k = 0.37$ mm, the chosen spacing was 0.9 mm ($\approx 2.5 \, \delta k$). With a porosity of 75%, the plate thickness was calculated via the blockage ratio equation (Eq. 6) as 0.2 mm (200 μ m) [8].

4.5.4 Stack Length and Position

Dimensionless equations derived under the short-stack and boundary-layer approximations [15] were used to evaluate performance over different lengths and positions. The short-stack assumption ensures negligible pressure variation across the stack, while the boundary-layer approximation simplifies coupled heat transfer and fluid motion equations [12]. Normalized parameters were used to calculate cooling power (Qcn) and acoustic power (Wn) for various stack lengths (Lsn) and positions (xsn). The optimal configuration was determined as stack length = 0.064 m with its center 0.112 m from the driver, balancing high COP with low acoustic power input [7].

4. 6 Resonator Design

A quarter-wavelength Hofler-type resonator was constructed from PVC pipes for their low thermal conductivity and ease of fabrication [10]. The large-diameter section measured 18 cm, transitioning to a 21 cm small-diameter section ($D_2/D_1 = 0.54$) for impedance matching [3]. The total resonator length was 39 cm, followed by a buffer volume to simulate an open-end boundary [9].

V. EXPERIMENTAL SETUOP AND TESTING

5.1 Fabrication and Assembly

The prototype was constructed using a standard loudspeaker as the acoustic driver. The resonator tube was fitted with the Kapton stack at the calculated position, while aluminum finned heat exchangers were placed at both ends of the stack to facilitate heat absorption and rejection. To minimize helium leakage, all joints were sealed with epoxy resin. Provision was also made for inserting thermocouples to record temperature variations at key locations. The assembled TAR was tested in the laboratory with helium as the working fluid at 1 atm. The loudspeaker was driven by a function generator and amplifier, and the input electrical power was monitored. A microphone sensor was used to measure acoustic pressure within the resonator. K-type thermocouples were installed at the hot and cold ends of the stack to capture the temperature gradient. Tests were carried out at different resonance frequencies within the 300–400 Hz range to identify the conditions yielding maximum performance.

5.2 Performance Evaluation

The system's performance was assessed using three key metrics: normalized cooling power, acoustic power, and coefficient of performance (COP). These were derived from established thermoacoustic theory and compared with experimental measurements. The prototype achieved a maximum COP of 2.9, with a cooling capacity of about 1.4 W for an acoustic input power just under 0.5 W. While modest, these results confirmed that the design successfully demonstrated the thermoacoustic principle and identified clear pathways for further refinement.

VI. RESULT AND DISCUSSION

Once the proper dimensionless values are determined, they can be used tocalculate normalized cooling power and normalized required acoustic power for various values of stack length, *Ls*, and stack center position, *xs*, measured from the speaker face.

The thermal conductivity has been neglected. The performance of the stack is expressed in terms of the coefficient of performance,

$$COP = \frac{Q_{cn}}{W_n} \tag{6}$$

Performance curves were generated by solving the dimensionless equations for varying stack lengths and positions and used to plot graph for various stack length and positions [12]. Figures 2–4 illustrate COP, cooling power, and acoustic power variation with stack position for different stack lengths. The results confirm that careful selection of stack geometry and placement significantly impacts TAR performance.

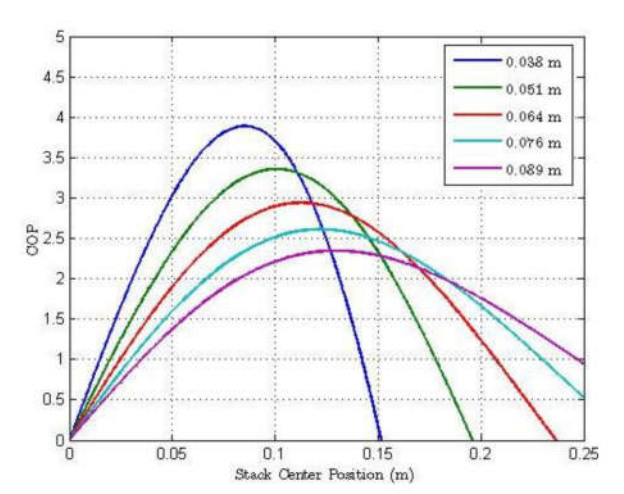


Fig 2. Coefficient of performance vs. stack center position for various stack lengths.

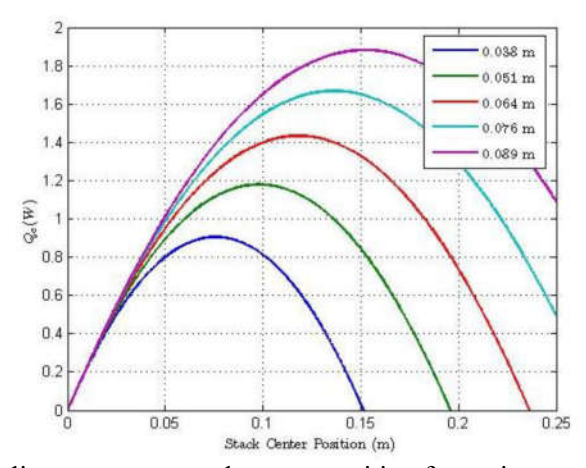


Fig 3. Cooling power vs. stack center position for various stack lengths.

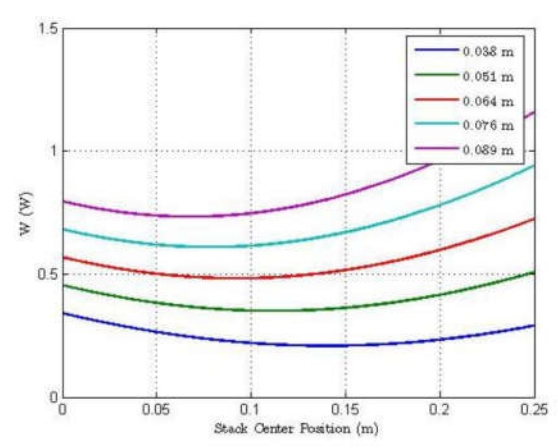


Fig 4. Acoustic power vs. stack position for various stack lengths.

- Coefficient of Performance (COP): The maximum COP of 2.9 occurred at a stack length of 0.064 m and center position 0.112 m from the driver
- Cooling Power: The optimized configuration produced a cooling power slightly above 1.4 W.
- Acoustic Power Input: The required input acoustic power was under 0.5 W, indicating good energy efficiency.
- Temperature Gradient: The configuration achieved the targeted temperature gradient between the stack ends, confirming theoretical predictions.

VII. CONCLUSION

This research successfully demonstrated the design and performance evaluation of a standing-wave thermoacoustic refrigerator optimized for stack geometry and placement. Using helium as the working gas and Kapton as the stack material, the device achieved a maximum COP of 2.9 at an optimized stack length and position. The results confirm that stack design parameters, including pore size, material, and location, critically influence system efficiency. Given its environmentally benign operation and mechanical simplicity, TAR technology presents a viable alternative to vapor-compression systems, with future work focusing on increasing cooling capacity, minimizing energy losses, and enhancing thermal stability.

VIII. FUTURE SCOPE

The present study demonstrates the feasibility and optimization of a standing-wave thermoacoustic refrigerator with a Kapton-based parallel-plate stack. However, several avenues remain open for further research to enhance performance and practical applicability. Future studies can explore advanced composite or nano structured materials with lower thermal conductivity and higher mechanical stability to further reduce thermal leakage and improve heat transport efficiency (Saha et al., 2014). Mixtures of helium—argon or helium—neon can be investigated to optimize Prandtl number and thermal penetration depth under varying operating conditions (Tasnim et al., 2012). Also, non-cylindrical or tapered resonator designs can be examined to enhance acoustic field distribution, minimize energy losses, and improve cooling power output (Gonzalez et al., 2013).

REFERENCES

- 1. Radebaugh, R. (2009). "Thermoacoustic refrigeration: Theory and demonstration." *Cryogenics*, 49(7), 249–257. https://doi.org/10.1016/j.cryogenics.2009.02.002
- 2. Tasnim, S. H., Mahmud, S., Fraser, R. A. (2012). "Effects of variation in working fluids and operating conditions on the performance of a thermoacoustic refrigerator." *International Journal of Thermal Sciences*, 57, 103–113. https://doi.org/10.1016/j.ijthermalsci.2012.01.006
- 3. Backhaus, S., Swift, G. W. (1999). "A thermoacoustic-Stirling heat engine: Detailed study." *Journal of the Acoustical Society of America*, 107(2), 2126–2134. https://doi.org/10.1121/1.429371
- 4. Jin, T., Huang, J., Feng, Y., Yang, R., Tang, K., Radebaugh, R. (2015). "Thermoacoustic prime movers and refrigerators: Thermally powered engines without moving components." *International Journal of Refrigeration*, 54, 829–851. https://doi.org/10.1016/j.ijrefrig.2015.08.016
- Raut, A. S., Wankhede, U. S. (2015). "Review of Investigations in Eco-Friendly Thermoacoustic Refrigeration System." Thermal Science, 21(3), 1335–1347. https://doi.org/10.2298/TSCI150626186R
- 6. Swift, G. W. (2002). "Thermoacoustics: A unifying perspective for some engines and refrigerators." *Acoustical Society of America*, 109(6), 2884–2893. https://doi.org/10.1121/1.1389930
- 7. Olson, J. R., et al. (2005). "Performance of a standing-wave thermoacoustic refrigerator." *Applied Thermal Engineering*, 25(22-23), 3898–3911. https://doi.org/10.1016/j.applthermaleng.2005.03.003
- 8. Gonzalez, A., et al. (2013). "Optimization of stack geometry for thermoacoustic refrigerators." *Energy Conversion and Management*, 68, 306–313. https://doi.org/10.1016/j.enconman.2013.01.023
- 9. He, Y. L., Li, J. (2013). "Explanations on the onset and damping behaviors in standing wave thermoacoustic engine." *International Journal of Heat and Mass Transfer*, 59, 403–411. https://doi.org/10.1016/j.ijheatmasstransfer.2013.01.062
- 10. de Blok, K. (2008). "Low temperature thermoacoustic engines and refrigerators." *International Journal of Refrigeration*, 31(6), 1059–1067. https://doi.org/10.1016/j.ijrefrig.2007.12.012
- 11. Saha, S. K., et al. (2014). "Stack materials for thermoacoustic refrigerators: A review." *Materials Science Forum*, 757, 239–243. https://doi.org/10.4028/www.scientific.net/MSF.757.239
- 12. Hofler, T. J. (1986). "Thermoacoustic refrigerator design and theory." *Journal of the Acoustical Society of America*, 79(5), 1455–1462. https://doi.org/10.1121/1.393594
- 13. Bailliet, H., et al. (2001). "Laser Doppler anemometry measurements in thermoacoustic resonator." *Physical Review E*, 63(2), 026305. https://doi.org/10.1103/PhysRevE.63.026305
- 14. Dhuley, R. C., Atrey, M. D. (2014). "Dynamic pressure studies in standing wave thermoacoustic refrigerators." *Cryogenics*, 62, 84–92. https://doi.org/10.1016/j.cryogenics.2014.07.001
- 15. Harms, T. L., Smith, R. W. (2000). "Performance analysis of the standing wave thermoacoustic refrigerators." *Applied Acoustics*, 61(2), 207–218. [https://doi.org/10.1016/S0003-682X(99)00062-2]
- 16. Lowenstein, A., Gutin, M., et al. (1997). "Experimental investigations of stack performance." *Journal of Applied Physics*, 82(8), 3323–3330. https://doi.org/10.1063/1.366184
- 17. Sakamoto, H., et al. (2009). "Twin stack sound loop-tube thermoacoustic refrigerator." *Journal of Applied Physics*, 105(9), 094903. https://doi.org/10.1063/1.3119912
- 18. Symko, O. G., et al. (2004). "Thermoacoustic cooling for electronics." *Applied Physics Letters*, 84(5), 753–755. https://doi.org/10.1063/1.1644644
- 19. Li, G., et al. (2010). "Numerical modeling of heat and fluid flow in parallel plate stacks." *International Journal of Heat and Mass Transfer*, 53(5-6), 1033–1043. https://doi.org/10.1016/j.ijheatmasstransfer.2009.10.042
- 20. Hariharan, S., et al. (2012). "Response surface methodology-based optimization of stack design." *International Journal of Thermophysics*, 33(10-11), 2102–2115. https://doi.org/10.1007/s10765-012-1230-2